Analyst

Native Mass Spectrometry Beyond Ammonium Acetate: Effects of Nonvolatile Salts on Protein Stability and Structure

Journal:	*Analyst*
Manuscript ID	AN-ART-02-2019-000266.R1
Article Type:	Paper
Date Submitted by the Author:	07-Mar-2019
Complete List of Authors:	Xia, Zijie; University of California, Berkeley DeGrandchamp, Joseph; University of California Berkeley Williams, Evan; University of California, Berkeley

Native Mass Spectrometry Beyond Ammonium Acetate: Effects of Nonvolatile Salts on Protein Stability and Structure

Zijie Xia, Joseph B. DeGrandchamp, and Evan R. Williams*

Department of Chemistry, University of California, Berkeley, California 94720-1460

Submitted to: *Analyst*

Date: Feb 6th, 2019

*Corresponding Author: Evan R. Williams

Phone: (510) 643-7161

e-mail: erw@berkeley.edu

Abstract

Native mass spectrometry is widely used to probe the structures, stabilities, and stoichiometries of proteins and biomolecular complexes in aqueous solutions, typically containing volatile ammonium acetate or ammonium bicarbonate buffer. In this study, nanoelectrospray emitters with submicron tips are used to produce significantly desalted ions of RNase A and a reduced, alkylated form of this protein, RA-RNase A, from solutions containing 175 mM ammonium acetate, as well as sodium chloride and Tris containing solutions with the same nominal ionic strength and pH. The charge-state distributions formed by nanoelectrospray ionization and tyrosine fluorescent emission data as a function of temperature from these solutions indicate that the folded form of RA-RNase A *in solution* is stabilized when ammonium acetate is replaced by increasing quantities of NaCl and Tris. Ion mobility data for the 7+ charge state of RA-RNase A indicates that the protein conformation in ammonium acetate changes with increasing concentration of NaCl which favors more compact structures. These results are consistent with observations reported 130 years ago by Hofmeister who found that ion

identity can affect the stabilities and the structures of proteins in solution. This study indicates the importance of buffer choice when interpreting native mass spectrometry data.

Introduction

Native mass spectrometry (MS) is widely used to transfer intact biological molecules and macromolecular complexes from buffered aqueous solutions in which the analytes are thought to have native or native-like structures into the gas phase for analysis by mass spectrometry.[1–3] Since the detection of noncovalent protein-ligand interactions using electrospray ionization (ESI) MS was first reported in the early

1990's,[4] there have been many demonstrations that elements of solution-phase biomolecule structures can be kinetically trapped and maintained in the gas phase without solvent.[5,6] Thus, information about structures and stabilities of biological molecules *in solution* can be probed using many different powerful gas-phase techniques. The stoichiometries of protein or other biomolecule complexes can be readily determined from mass measurements, making native mass spectrometry well suited for investigating kinetics and thermodynamics of macromolecular complex assemblies as well as providing information about intermediates in disease-related protein aggregates, such as αβ aggregates.[2,7] In combination with collisional activation and ion mobility spectrometry, information about the number and stabilities of different domains within proteins has been obtained.[8–10] Native MS has been extended to membrane proteins through the use of solubilizing detergents, which can be released from the proteins by collisional activation in the gas phase.[11]

Volatile buffers, such as ammonium acetate and ammonium bicarbonate, are predominantly used in native MS to provide the necessary ionic strength and pH for proteins and protein complexes to fold and assemble.[2] In contrast, the intracellular and

the extracellular environments surrounding proteins and complexes contain many nonvolatile salts, consisting of ions such as sodium, potassium, phosphate, and chloride, with concentrations of tens to hundreds of millimolar.[12] Many different buffers are commonly used to mimic physiological conditions in order to maintain the structures and functions of proteins and protein complexes. Common biochemical buffers for protein preparations, such as Tris buffer and phosphate buffered saline, contain on average 100 mM to 200 mM of nonvolatile salts. However, high concentrations of nonvolatile salts are a bain to native MS because they adversely affect accurate mass measurements and signal. Nonvolatile salts adduct onto protein ions causing the mass spectral peaks to broaden, resulting in loss of resolution, mass measuring accuracy, and sensitivity. Salt adduction decreases sensitivity by spreading the protein ion signal over multiple different masses, and salt clusters can increase baseline noise and cause ion suppression of the analytes of interest.[13,14] Concentrations of nonvolatile salts greater than 100 mM can lead to broad, unresolved peaks in a mass spectrum from which no mass information is typically obtained with common biochemical buffers.[15,16]

Methods in native MS to desalt protein ions from the solutions with nonvolatile salts by adding a low concentration of desalting agents into solution[14,17–19] or in the gas phase have been developed.[20] Although these methods are effective at producing gaseous ions exhibiting significantly reduced levels of salt adduction for solutions with lower than 25 mM nonvolatile salts, this is far short of physiological conditions and the concentration of nonvolatile salts in common biochemical buffers. As a result, aqueous protein solutions are typically buffer exchanged from nonvolatile buffers to volatile buffers before native MS by using methods such as dialysis,[21] diafiltration[22] or ion chromatography.[2] This process, however, changes the solution environment of the biological molecules and complexes. For protein and protein complexes that require a specific nonvolatile salt for proper folding and function, buffer exchange into ammonium acetate can result in loss of structural information. For example, NtrC4 (activator protein) from *Aquifex aeolicus* needs millimolar concentrations of some nonvolatile salts to form a hexamer that dominates in physiological conditions. In ammonium acetate solution without these salts, the heptamer of NtrC4 is instead the dominant species.[23] Thus,

complete removal of nonvolatile salts in native MS can lead to changes in the stabilities of different protein complexes.[23,24]

More generally, it has been known for over 130 years that protein stability, solubility, and conformations depend not only on the ionic strength and pH of a solution but also on the identity of the constituent ions. This observation has led to what is known as the Hofmeister ion series in which both anions and cations are ordered based on their propensity to either stabilize or destabilize proteins in solution.[25,26] For example, guanidinium in the form of a chloride or thiosulfate salt is widely used to destabilize the native form of proteins and can lead to the denatured form being more stable at high salt concentrations.[27] Ammonium sulfate is often used to stabilize or "salt-out" the native form of proteins in order to form crystals suitable for crystallography.[28] The origin of the effect of ions on protein stability has been attributed to direct ion-protein interactions[26,27] and to ion-water interactions that can affect the hydrogen-bonding network of water molecules that surround the protein ions.[29,30] The latter effect is significant for higher charged anions in aqueous solutions, which affect hydrogen bonding networks of water molecules located remotely from the ion.[30] Effects of low concentrations of high valency

ions in methanol containing aqueous solution were shown to affect the gaseous conformations of misfolded concanavalin A ions and by inference, the solution-phase structure and therefore stability of the protein complex.[24]

We have recently introduced a new method that is sufficiently effective at desalting protein and protein complex ions during the ESI process that resolved charge-state distributions can be obtained directly from solutions containing high concentrations of nonvolatile salts.[15,16,31,32] Hence, analyte masses can be measured from traditional biochemical buffers without protein denaturation during the ESI process. This method uses submicron electrospray emitters to produce sufficiently small nanodrops that most of the nonvolatile salts are separated from analyte molecules during droplet formation.[16] Here, this method is used to investigate the effects of ammonium acetate, sodium chloride, and Tris buffers on protein stability and structure at solution concentrations that are typically used in studies of protein chemistry that employ other biochemical methods. Results from protein charge-state distribution and ion mobility arrival time measurements of reduced, alkylated RNase A indicate that both the conformation and the stability of the folded forms of this protein depend on the identity of the ions present

in solution. Temperature-dependent fluorescence measurements show that the thermal stability of this protein is different in ammonium acetate versus Tris buffer, consistent with the mass spectral results. These results demonstrate that there can be differences in the conformation and stability of a protein in ammonium acetate versus a more commonly used biochemical buffer solution. Thus, the choice of the solution environment can be important for interpreting native MS data.

Experimental Method

Mass Spectrometry

Mass spectrometry experiments are performed using a Waters SYNAPT G2Si mass spectrometer (Milford, MA). Electrospray emitters with an inner diameter of 0.66 ± 0.02 μm are pulled from borosilicate capillaries (1.0 mm o.d./0.78 mm i.d., Sutter Instruments, Novato, CA) using a Flaming/Brown micropipette puller (Model P-87, Sutter Instruments, Novato, CA). The emitter diameter is measured with a scanning electron microscope (Hitachi TM-1000 SEM, Schaumburg, IL). Protein ions are formed

from aqueous buffered solutions by applying 0.8 kV to 1.3 kV on a 0.127 mm diameter platinum wire that is inserted into the emitters and is in contact with the solution. The emitter tip is positioned ~5 mm away from the instrument entrance with a Z-spray configuration. The population of folded and unfolded forms of the protein is determined from the abundances of ions in the corresponding charge-state distribution.[33] These values were not corrected for possible differences in ionization efficiency or ion transmission/detection efficiency. Traveling wave ion mobility spectrometry (TWIMS) arrival time data are acquired using a wave velocity of 900 m/s, and a wave height of 40 V. Helium and ion mobility (nitrogen) gas flow rates are 180 mL/min and 90 mL/min, respectively. These TWIMS parameters were selected to minimize ion heating during TWIMS.[34] Ubiquitin, β-lactoglobulin, lysozyme, α-lactalbumin, ribonuclease A, ovalbumin and avidin ions, formed from 200 mM ammonium acetate (AA), are used to calibrate the arrival time data to obtain collisional cross sections using the procedure described previously by Ruotolo and et al. (Figure S-1).[35] The uncertainties reported on the collisional cross sections are based on the precision of three measurements on the same sample but do not reflect the accuracy of the measurements.

Protein Modification and Sample Preparation

Reduced and alkylated bovine pancreatic ribonuclease A is prepared as previously described[36] by dissolving lyophilized powder of ribonuclease A in 200 mM ammonium acetate (pH 8.8) solutions containing 6 M guanidine hydrochloride, 15 mM dithiothreitol, and 80 mM iodoacetamide. The reaction is incubated in the dark for approximately two hours. The reaction solution is buffer exchanged into 175 mM AA with a Biospin column (Bio-Rad, Hercules, CA). The final concentration of reduced/alkylated RNase A stock solution is ~200 μM. Lyophilized protein powders of ubiquitin, β-lactoglobulin, bovine pancreatic ribonuclease A (RNase A), cytochrome *c*, ovalbumin, avidin, ammonium acetate, Tris hydrochloride, NaCl, guanidine hydrochloride, dithiothreitol, and iodoacetamide are from Sigma (St. Louis, MO). All buffer solutions containing various concentrations of ammonium acetate, sodium chloride, and Tris are pH adjusted with ammonium hydroxide and acetic acid to pH 6.8 ±0.3. 10 μM protein samples are prepared by diluting protein stock solution with pH adjusted buffers.

Tyrosine Fluorescence

Tyrosine fluorescence emission spectra of reduced, alkylated RNase A in 175 mM AA, 25 mM AA with150 mM NaCl, and 25 mM Tris with 150 mM NaCl are obtained with a FluoroMax-3 spectrometer (Horiba Scientific, Kyoto, Japan). The samples are excited at 280 nm, and the emission spectra are scanned from 290 nm to 400 nm. The slits widths for both excitation and emission are 3 nm. Each sample is heated from 25 °C to 77.5 °C (± 0.2 °C tolerance) in 2.5 °C increments. The solutions are equilibrated for five minutes at each temperature before emission spectra are measured. Three emission spectra are obtained, background subtracted, and averaged for each sample at each temperature.

Tyrosine emission intensity of reduced, alkylated RNase A and a short peptide (AAAYGGF) in 175 mM AA, 25 mM AA with150 mM NaCl, and 25 mM Tris with 150 mM NaCl are obtained with a multi-mode microplate reader (Synergy H4 hybrid reader, BioTek, Winooski, VT) in 384-well polystyrene solid black low volume flat bottom microplates (Corning, New York, NY). The plate reader is operated at the top reading

mode. Each protein/peptide sample is measured five times, averaged and background subtracted in emission acquisition mode with 280 nm ±10 nm excitation and 302 ±10 nm emission at 25 °C ± 0.2 °C.

Results and Discussion

Solution Ion Effects on RA-RNase A Stability and Structure.

Effects of different salts on the ESI mass spectra of reduced, alkylated bovine pancreatic ribonuclease A (RA-RNase A) were investigated from solutions with the same nominal ionic strength (175 mM) and pH (6.8) but containing different concentrations of AA, NaCl and Tris buffer. RA-RNase A has at least two distinct conformations or families of unresolved conformers that coexist in solution corresponding to folded and unfolded forms, making this an ideal system to investigate effects of ion identity on conformational energetics.[32,36] A representative mass spectrum from 175 mM AA is shown in Figure 1a. The charge-state distribution of RA-RNase A is bimodal with a distribution of high charge states between 10+ and 14+, indicating a largely unfolded structure, and a distribution of lower charge states between 6+ and 9+,

consistent with a molten globular or more compact structure. Results from circular dichroism (CD),[37] hydrogen-deuterium exchange,[38] and X-ray scattering[39] indicate that the RA-RNase A has a structure that is close to either a random coil or a molten globule depending on solution composition, pH, and temperature. For example, CD results indicate that about 66% of the structure of RA-RNase A is random coil in 50 mM phosphate buffer (pH 6).[37] The mass spectrometry results from 175 mM AA also indicate substantial random coil structure, but native mass spectrometry has the advantage that it is able to reveal two coexisting structures in solution that are not identified by CD. There is also signal for intact (not reduced) RNase A, which appears at just the lower charge states 6+ to 8+. There are no high charge states of RNase A, indicating that this protein is essentially fully folded. The four internal disulfide bonds of RNase A constrain the protein, so it cannot adopt as a fully unfolded form as RA-RNase A. The lower charge-state distribution of RA-RNase A is similar to the charge states of RNase A, indicating that the conformation of RA-RNase A at lower charge states is largely compact or similarly folded as RNase A. The abundance of the folded form of

RA-RNase relative to the unfolded form is estimated to be ~58% ± 3% based on the abundances of ions that make up the two respective charge-state distributions.

Results obtained from solutions in which 10 mM of AA is replaced by 10 mM of NaCl are shown in Figure 1b. The ion signal in the lower charge states is significantly broadened owing to sodium ion adduction, but the high charge state ions are notably less adducted, consistent with earlier reports of more sodium ions adducting to low charge states of a protein.[40,41] Although the peaks in the lower charge-state distribution are significantly broadened, the integrated abundances of charge states in the high and low charge-state distributions indicate that there is a similar fraction of the unfolded form of the protein (~55% ± 2%) as there is for the solution with no NaCl (~58% ± 3%; Figure. 1a).

For solutions in which 50 mM of AA is replaced by the same concentration of NaCl, the mass spectra show significantly broadened peaks in both distributions corresponding to more heavily adducted folded and unfolded conformers (Figure 1c). Moreover, the abundance of the lower charge-state distribution is significantly enhanced over that of the high charge-state distribution despite the more adducted, broader peaks

in the former. Shifts in the average charge of both distributions are also apparent with the higher charge-state distribution shifting slightly to lower charge and the lower charge-state distribution shifting slightly to higher charge. Based on the integrated abundances of the ions in these two distributions, the relative abundance of the unfolded form of RA-RNase A is ~37% ± 10%.

The mass spectra from solutions consisting of 25 mM AA and 150 mM NaCl (Figure. 1d) are notably different from those obtained from solutions with significantly less NaCl. There is predominantly one charge-state distribution, and the center of this distribution is shifted to even higher charge than that of the folded population with 50 mM NaCl (Figure 1c). The population of unfolded conformers is significantly reduced compared to that of solutions with lower NaCl concentrations. The relative abundances of the high charge states (10+ to 14+) indicate that only ~16% ± 3% of the RA-RNase A population is unfolded. The decreasing abundance of the high charge-state distribution relative to the lower charge-state distribution with increasing NaCl concentration indicates that the folded form of RA-RNase A is stabilized with increasing NaCl despite the nearly identical ionic strength and pH of these solutions. The shift in the center of

the charge-state distribution to higher charges for the folded form of RA-RNase A in 150 mM NaCl and 25 mM AA compared to that in 175 mM AA alone suggests that the conformation of the protein may differ in these two solutions. It should be noted that sodium adduction to the ions does not appear to be responsible for the increased charging of the folded form because sodium adduction to the unfolded form results in lower charge states. Thus, the changes in charge-state distributions likely reflect a change in solution conformation.

Replacing 25 mM AA with 25 mM Tris in solutions containing 150 mM NaCl results in a predominant charge-state distribution at lower charges (6+ to 9+). Higher charge states (10+ to 14+) are formed to some extent, but their abundance is difficult to quantitate because of the high baseline chemical noise as a result of unresolved salt clusters. After baseline subtraction, the abundance of these higher charges states relative to the low charge states is only ~3% ± 4%. These results indicate that RA-RNase A adopts a predominantly folded conformation in solutions of 25 mM Tris and 150 mM NaCl.

The concentration of sodium chloride in the Tris buffer and that in 25 mM AA with 150 mM NaCl is the same and the extent of adduction to the folded forms of these ions is similar (Figure 1d and e, respectively), yet the charge-state distributions differ. These results provide further evidence that the difference in charge-state distributions observed for these two solutions reflects differences in conformations of the folded form of the protein.

The solution composition can potentially affect other factors, such as droplet temperature or ionization efficiency. In a previous study, ~300 nm theta emitters produce initial droplets that are fully desolvated before the droplets enter the instrument due to their short lifetime (~1 μs).[42] Droplets from a 500 nm single barrel emitter are likely to be only slightly larger and should also lead to gaseous ion formation prior to the mass spectrometer so effects of the heated interface should be negligible. Droplets formed from these different aqueous solutions have similar surface tensions and should have similar extents of charge. Thus, energy transferred to the droplets from collisions as a result of acceleration outside of the mass spectrometer and the resulting droplet temperature should not be significantly affected by these different solution compositions.

The quality of the mass spectra from solutions consisting of more than 50 mM NaCl (Figure 1c-e) appears poor compared to those obtained from solutions with significantly less NaCl. The background is high owing to the chemical noise of various salt clusters that are typically below m/z ~4000, which can interfere with small protein ions in this same m/z range. Moreover, preliminary results indicate that the extent of adduction onto protein ions formed with a single emitter tip size is roughly related to protein surface areas. Thus, the desalting effects of small emitters are generally more prominent for larger protein complexes owing to their lower surface area-to-mass ratios and the formation of ions above m/z 3000 which reduces effects of chemical noise from salt clusters. Despite the broad mass spectral peaks, the conclusions about the effects of high concentrations of nonvolatile salts on the relative stability of the unfolded and folded forms of this protein, which are determined from the relative abundances of the corresponding charge-distributions, can still be deduced from these data.

Effects of Different Ions on RA-RNase A Thermal Stability in Solution.

In order to investigate the effects of different ions on the solution-phase thermal stability of RA-RNase A, tyrosine fluorescence emission spectra were obtained for this protein in three solutions consisting of 1) 175 mM AA, 2) 25 mM AA and 150 mM NaCl, and 3) 25 mM Tris and 150 mM NaCl at temperatures between 25 °C and 77.5 °C. The emission peak of RA-RNase A is broad, centered around 302 nm, and the intensity at 302 nm generally decreases with increasing temperature (Figure. 2). The gradual decrease in fluorescence emission intensity with increasing temperature is attributed to competitive non-radiative deactivation pathways at higher temperatures.[43,44] The emission intensity of tyrosine fluorescence is also influenced by the environment that surrounds the six tyrosine residues (Tyr-25, Tyr-73, Tyr-76, Tyr-92, Tyr-97, Tyr-115) in the protein, including both solvent accessibility as well as proximity to other residues. Three tyrosine residues in RNase A, Tyr-25, Tyr-73, and Tyr-97, are buried inside the protein interior whereas the other three are partially exposed to the solvent based on the structure obtained through NMR and X-ray crystallography.[45,46] Thus, these measurements monitor local changes around tyrosine residues rather than more global measures of protein conformational change. As a result, a sigmoidal melting curve often

characteristic of protein melting data obtained from other methods, such as CD, does not always occur with tyrosine fluorescence emission. CD was not used in these experiments because of interference from ammonium acetate at high concentration.

The temperature dependent emission data from the three solutions show differences in both fluorescent emission intensity and temperature dependence. The emission intensity of RA-RNase in 175 mM AA is consistently lower than that of the two solutions containing 150 mM NaCl. This difference in intensity can be attributed to either differences in solution composition and/or differences in protein conformation.[45] In order to determine how different ions in solution might affect the emission intensity of tyrosine, the emission intensity of a short tyrosine-containing peptide (AAAYGGFL) was measured from the three solutions at 25 °C. This peptide was chosen because tyrosine has neighboring residues and is not expected to have a particularly stable folded form. The tyrosine is also remote from the C- and N- terminus to avoid any effects of charge on tyrosine fluorescence. The emission intensity of tyrosine at 302 nm in both solutions containing AA is similar, but the emission in 25 mM Tris and 150 mM NaCl is slightly higher (*SI Appendix*, Table S1). This indicates that AA interacts with the tyrosine side

chain and results in fluorescent quenching. Acetate is a proton acceptor that has been reported previously to quench tyrosine fluorescence.[45,47].

The emission intensity of tyrosine in RA-RNase A in 25 mM AA and 150 mM NaCl is consistently higher than that in 175 mM AA, whereas the emission intensity from AAAYGGFL is essentially the same in these two solutions (Figure 2 and Table S-1). This result suggests that the differences in fluorescence intensity of RA-RNase A are not due to quenching by different ions in solution but rather due to conformational differences throughout this temperature range. Moreover, the trend of emission intensity with increasing temperature is different at temperatures above 65 °C with these three solutions (Figure 2). In solutions containing 175 mM AA or 25 mM AA and 150 mM NaCl, the intensity increases slightly between 65 °C and 75 °C and decreases rapidly at higher temperatures. In contrast, the signal for the solution with 25 mM Tris and 150 mM NaCl increases between 67.5 °C and 72.5 °C before decreasing at higher temperatures. The signal rise is higher and is shifted by ~2.5 °C compared to that for the other two solutions.

An increase in the tyrosine emission intensity also occurs for RNase A in this temperature range. This phenomenon was attributed to an increase in distance between disulfide bonds and two tyrosine residues that occurs upon unfolding at ~62 °C in 10 mM phosphate buffer (pH 7), which decreases the extent of fluorescence quenching by the disulfide bonds.[45] The similar trend in fluorescence emission with temperature for both native RNase A and RA-RNase A indicates that the alkylated cysteine residues may also quench emission and that the folded structure of RA-RNase A has similar contacts as RNase A in these regions. This result and the similar charge-state distributions suggest that many other regions of the folded form of RA-RNase A may be similar to that of RNase A as well. Both the higher emission intensity at elevated temperatures and the shift in fluorescence intensity between 67.5 and 72.5 °C observed from the Tris/NaCl solution indicates that RA-RNase A is more stable in this solution. The emission data also suggest that the conformation in this solution may be closer to that of native RNase A than the other two solutions, which is consistent with the mass spectral results.

Ion Mobility and Ion Effects on Solution Structure.

Both the mass spectral data and the tyrosine emission temperature melt data indicate that the folded form of RA-RNase A is more stable (relative to the unfolded or random coil form) in a solution consisting of 25 mM Tris and 150 mM NaCl than it in a 175 mM AA solution. Also, the shift in the charge states corresponding to the folded form of RA-RNase A with increasing NaCl and with Tris suggests that the actual conformation of the folded form of the protein is affected by these different ions, which is consistent with the fluorescence data as well. To investigate the structures of the folded form of the protein in solutions with various concentrations of AA and NaCl, ion mobility data was acquired for the 6+ and 7+ ions under conditions identified in Figure 1. Because ion conformation can depend on charge state, the same charge states produced from the different solutions are compared.[48] Gas-phase protein ion conformations can also depend on the number and the identity of salt adducts. Adducted ions are typically more compact [48,49] and are also more stable in the gas phase.[50,51] For cations, these effects become more apparent with increasing number of adducts and higher valency salts.[48,51] For this reason, a relatively narrow mass window

was chosen to isolate the precursors that are either fully protonated or have up to two sodium adducts in this study. This low level of sodium adduction is expected to have minimal effect on protein structure.[48]

Arrival time data from traveling wave ion mobility spectrometry (TWIMS) measurements for the 7+ charge state of RA-RNase A formed from 175 mM AA is shown in Figure 3a. There is an abundant peak (~90 %) at 13.7 ± 0.1 ms and a much less abundant peak (~10 %) at 11.3 ± 0.2 ms. These data indicate that the 7+ ion has at least two gas-phase conformations (or families of conformers) that can be distinguished by ion mobility. By calibrating these arrival time data (Figure S-1), an average collisional cross section of 1562 ± 7 $Å^2$ and 1392 ± 15 $Å^2$ are obtained for the major and minor conformers, respectively. There are also two peaks in the arrival time distributions of 7+ intact RNase A corresponding to two conformers with cross sections of 1496 ± 5 $Å^2$ (~ 92%) and 1365 ± 7 $Å^2$ (~ 8%). The minor conformers for both RA-RNase A and RNase A have cross sections that are similar to the value reported from radio-frequency confining drift tube ion mobility measurements of RNase A (1340 $Å^2$; 200 mM AA; pH 7),[52] but the minor conformer of RA-RNase A is slightly larger than that of RNase A. The

major conformers of both proteins have a much larger cross section, but the cross section of RA-RNase A is again larger than that of RNase A, consistent with a slightly more unfolded form of the reduced species in this solution. TWIMS measurements under identical solution conditions to those reported previously result in the same cross sections as those measured in 175 mM AA indicating that the ions may be heated somewhat in these TWIMS measurements. By comparison, the cross section of the 6+ ion is 1313 ± 3 $Å^2$ for RA-RNase A and 1282 ± 3 $Å^2$ for RNase A, which is consistent with the reported value 1290 $Å^2$ for RNase A (Figure S-2 and S-3).[52] The collisional cross section for the 6+ charge state of RA-RNase is slightly larger and may be attributable to its higher mass and hence volume. Conformations of gaseous protein ions can be influenced by instrument conditions. A similar heating effect has been reported for other proteins with charge states close to the transition observed between folded and unfolded forms using TWIMS.[34,53] It is interesting that the more compact structure or structures of RA-RNase A have collisional cross sections that are similar to that of native RNase A, indicating that the more compact structures of RA-RNase A may closely resemble the native form of the protein.

The ion mobility arrival time data for RA-RNase A 7+ in solutions with 10 mM NaCl and 50 mM NaCl are shown in Figure 3b and 3c, respectively. Both similarly compact and a less compact structure are observed from these NaCl containing solutions, but the relative abundance of the more compact structure is significantly increased when NaCl is present. The collisional cross section of the more compact conformation (arrival time ~11 ms) is also slightly smaller from the solutions containing NaCl than it is from 175 mM AA. The more compact conformation has a collisional cross section of 1353 ± 8 $Å^2$ from the solutions with 10 mM NaCl or 50 mM NaCl compared to 1397 ± 21 $Å^2$ from 175 mM AA. The results in Figure 3 indicate that the population of more compact protein structures increases with increasing NaCl in the aqueous solution. Because the same charge state ions with a similar number of sodium adducts are compared, these results indicate that the solution-phase conformations of the folded form of RA-RNase A are different in solutions containing higher concentrations of NaCl from those containing just AA. Ion mobility data for the RA-RNase A 6+ charge state shows a single peak for the protein corresponding to a collisional cross section of 1302

± 3 Å^2 from each of these solutions, which is consistent with the reported value for RNase A 6+ ion. (Figure S-3).[52]

A key challenge in interpreting ion mobility data for solutions containing NaCl concentrations above 50 mM is interference from large salt clusters, including multiply charged clusters, which increase significantly in abundance and complexity with salt concentration. The arrival times of some of these salt clusters in the selected *m*/*z* window can overlap with those of the protein conformers. Below 50 mM, these interferences are relatively minor and the arrival times do not overlap significantly with those of the protein conformers. For example, the normalized abundances in the arrival times of salt clusters generated from solutions without protein are also shown in Figure 3. The ion identity, abundances, and arrival times change with increasing NaCl concentration. When the concentration of NaCl is 50 mM or lower, the most abundant peak in the arrival time distribution of the salt solutions without protein does not appear to a significant extent in the distributions with the proteins. Moreover, these peaks appear at different arrive times indicating that these salt clusters do not interfere significantly with the ion mobility data for the protein ions.

At 150 mM NaCl with either 25 mM AA or 25 mM Tris, salt clusters overlap with protein signal to a large extent both in *m*/*z* and ion mobility arrival times. For the 7+ charge state, there is no significant overlap between salt clusters and protein in the region between ~11 and 13 ms for the 25 mM AA and 150 mM NaCl solution and between ~12 and 14 ms for the 25 mM Tris and 150 mM NaCl solution (Figure S-4 and Figure S-5). In these regions, there is an abundant signal for the 7+ ion. There is little apparent protein signal above 13.5 ms. These results indicate that a more compact form of the protein is favored in these solutions compared to 175 mM AA, but little additional information about the nature of these structures can be obtained from these experiments.

It is interesting that the ion mobility data for the 7+ ion indicates that there is compaction in structure with increasing NaCl concentration, yet the distribution of lower charge states shifts to slightly higher charge. This phenomenon may be due to the incomplete folding of higher charge state population that is formed at low or no NaCl resulting in the slightly higher charge states in the lower charge-state distribution. The formation of intermediates along the folding and unfolding pathways have been

observed for many different proteins.[54,55] It should also be noted that a reduction of the collisional cross section can be accompanied by an increase in charge as a result of a change in molecular shape which favors more charge separation.[56]

Conclusion

Native mass spectrometry of soluble proteins is nearly exclusively performed from volatile aqueous buffered solutions consisting of either ammonium acetate or ammonium bicarbonate. These conditions are not typically used to investigate the structures and the functions of proteins or macromolecular complexes using other methods. A key question is how the identity of different ions that make up the necessary ionic strength of a solution may affect the interpretation of native MS data obtained from different solutions. For RA-RNase A, mass spectral charge-state distributions and tyrosine fluorescence data as a function of temperature indicate that the folded form of the protein is stabilized by replacing ammonium acetate with NaCl and Tris for solutions with the same nominal ionic strength and pH. Moreover, the charge-state distributions and ion mobility data for the 7+ ion indicate that the conformation of the folded protein

differs in these solutions where AA is replaced with NaCl. Thus, both the structure and the stability of this protein is different in solutions containing high levels of NaCl compared to those in just AA.

In cases where the folded form of a protein is much more stable, effects of different ions on the stabilities and structures of proteins and protein complexes are likely to be much less apparent. Thus, in numerous cases documented in the literature, native mass spectrometry using ammonium acetate or ammonium bicarbonate leads to conclusions about structure and stability comparable to those obtained by other methods from solutions that more accurately mimic either the intracellular or the extracellular environment. However, when there are multiple conformers of a protein or multiple stoichiometries for protein complexes in solution, differences in the stabilities are much lower, and the identity of the constituent ions in solution will likely make a difference in the forms and structures of the proteins formed from these solutions in native mass spectrometry.[23,24] Very recent studies using submicron emitter tips with mass spectrometry indicate that the stoichiometries and the stabilities of large protein complexes and protein-ligand complexes can also be affected by high concentrations of

nonvolatile salts.[55, 56] Mass spectrometry has the advantage that multiple conformers or forms of a complex can be readily identified based on charge-state distributions, masses, and ion mobility data. Native mass spectrometry can now be performed from a range of traditional biochemical buffers, including phosphate and Tris with >150 mM of Na^+ or K^+ using nanoelectrospray emitters with submicron tips. The use of such tips should be beneficial for native mass spectrometry of proteins and macromolecular complexes where multiple forms are present to better compare to other methods that use traditional biochemical buffers.

Acknowledgments

This material is based upon work supported by the National Science Foundation Division of Chemistry under grant number CHE-1609866. The authors are grateful for financial support from CALSOLV and also thank Dr. Anna Susa and Dr. Ethan McSpadden for helpful discussions.

Reference

1 J. A. Loo, *Int. J. Mass Spectrom.*, 2000, **200**, 175–186.

2 H. Hernández and C. V Robinson, *Nat. Protoc.*, 2007, **2**, 715–726.

3 A. C. Leney and A. J. R. Heck, *J. Am. Soc. Mass Spectrom.*, 2017, **28**, 5–13.

4 B. Ganem, Y. T. Li and J. D. Henion, *J. Am. Chem. Soc.*, 1991, **113**, 6294–6296.

5 D. S. Gross, Y. Zhao and E. R. Williams, *J. Am. Soc. Mass Spectrom.*, 1997, **8**, 519–524.

6 T. J. El-Baba, D. W. Woodall, S. A. Raab, D. R. Fuller, A. Laganowsky, D. H. Russell and D. E. Clemmer, *J. Am. Chem. Soc.*, 2017, **139**, 6306–6309.

7 T. J. Esparza, N. C. Wildburger, H. Jiang, M. Gangolli, N. J. Cairns, R. J. Bateman and D. L. Brody, *Sci. Rep.*, 2016, **6**, 38187.

8 J. L. P. Benesch, J. A. Aquilina, B. T. Ruotolo, F. Sobott and C. V. Robinson, *Chem. Biol.*, 2006, **13**, 597–605.

9 M. Zhou, S. Dagan and V. H. Wysocki, *Angew. Chemie Int. Ed.*, 2012, **51**, 4336–

4339.

10 Y. Zhong, L. Han and B. T. Ruotolo, *Angew. Chemie Int. Ed.*, 2014, **53**, 9209–9212.

11 A. Laganowsky, E. Reading, J. T. S. Hopper and C. V Robinson, *Nat. Protoc.*, 2014, **8**, 639–651.

12 K. Diem and C. Lentner, *Blood – Inorganic substances*, CIBA-GEIGY Ltd., Basle, Switzerland, 1970.

13 P. Pan and S. A. McLuckey, *Anal. Chem.*, 2003, **75**, 5468–5474.

14 A. T. Iavarone, O. A. Udekwu and E. R. Wiliams, *Anal. Chem.*, 2004, **76**, 3944–3950.

15 A. C. Susa, Z. Xia and E. R. Williams, *Angew. Chemie Int. Ed.*, 2017, 1–5.

16 A. C. Susa, Z. Xia and E. R. Williams, *Anal. Chem.*, 2017, **89**, 3116–3122.

17 T. G. Flick, C. a. Cassou, T. M. Chang and E. R. Williams, *Anal. Chem.*, 2012, **84**, 7511–7517.

18 D. J. Clarke and D. J. Campopiano, *Analyst*, 2015, **140**, 2679–2686.

19 C. A. Cassou and E. R. Williams, *Analyst*, 2014, **139**, 4810–4819.

20 J. C. Demuth and S. A. McLuckey, *Anal. Chem.*, 2015, **87**, 1210–1218.

21 F. Xiang, Y. Lin, J. Wen, D. W. Matson and R. D. Smith, *Anal. Chem.*, 1999, **71**, 1485–1490.

22 M. Prodanov, I. Garrido, V. Vacas, R. Lebrón-Aguilar, M. Dueñas, C. Gómez-Cordovés and B. Bartolomé, *Anal. Chim. Acta*, 2008, **609**, 241–251.

23 J. D. Batchelor, H. J. Sterling, E. Hong, E. R. Williams and D. E. Wemmer, *J. Mol. Biol.*, 2009, **393**, 634–643.

24 L. Han and B. T. Ruotolo, *Angew. Chemie - Int. Ed.*, 2013, **52**, 8329–8332.

25 F. Hofmeister, *Arch. Exp. Pathol. und Pharmakologie*, 1888, **24**, 247–260.

26 X. Tadeo, B. López-Méndez, D. Castaño, T. Trigueros and O. Millet, *Biophys. J.*, 2009, **97**, 2595–2603.

27 O. D. Monera, C. M. Kay and R. S. Hodges, *Protein Sci.*, 1994, **3**, 1984–1991.

28 P. Wingfield, in *Current Protocols in Protein Science*, John Wiley & Sons, Inc., Hoboken, NJ, USA, 1998, vol. Appendix 3, p. A.3F.1-A.3F.8.

29 B. Hribar, N. T. Southall, V. Vlachy and K. A. Dill, *J. Am. Chem. Soc.*, 2002, **124**, 12302–12311.

30 M. J. DiTucci and E. R. Williams, *Chem. Sci.*, 2017, **8**, 1391–1399.

31 A. C. Susa, J. L. Lippens, Z. Xia, J. A. Loo, I. D. G. Campuzano and E. R. Williams, *J. Am. Soc. Mass Spectrom.*, 2018, **29**, 203–206.

32 Z. Xia and E. R. Williams, *J. Am. Soc. Mass Spectrom.*, 2018, **29**, 194–202.

33 I. A. Kaltashov and S. J. Eyles, *Mass Spectrom. Rev.*, 2002, **21**, 37–71.

34 S. I. Merenbloom, T. G. Flick and E. R. Williams, *J. Am. Soc. Mass Spectrom.*, 2012, **23**, 553–562.

35 B. T. Ruotolo, J. L. P. Benesch, A. M. Sandercock, S.-J. Hyung and C. V Robinson, *Nat. Protoc.*, 2008, **3**, 1139–1152.

36 H. J. Sterling, C. A. Cassou, M. J. Trnka, A. L. Burlingame, B. A. Krantz and E. R. Williams, *Phys. Chem. Chem. Phys.*, 2011, **13**, 18288–18296.

37 S. Takahashi, T. Kontani, M. Yoneda and T. Ooi, *J. Biochem.*, 1977, **82**, 1127–33.

38 C. K. Woodward and A. Rosenberg, *Proc. Natl. Acad. Sci. U. S. A.*, 1970, **66**, 1067–74.

39 J. Jacob, R. S. Dothager, P. Thiyagarajan and T. R. Sosnick, *J. Mol. Biol.*, 2007, **367**, 609–615.

40 X. Yue, S. Vahidi and L. Konermann, *J. Am. Soc. Mass Spectrom.*, 2014, **25**, 1322–1331.

41 T. G. Flick, S. I. Merenbloom and E. R. Williams, *J. Am. Soc. Mass Spectrom.*, 2011, **22**, 1968–1977.

42 Z. Xia and E. R. Williams, *Analyst*, 2019, **144**, 237–248.

43 S. W. Allison and G. T. Gillies, *Rev. Sci. Instrum.*, 1997, **68**, 2615–2650.

44 J. A. Gally and G. M. Edelman, *Biochim. Biophys. Acta*, 1962, **60**, 499–509.

45 M. Noronha, J. C. Lima, E. Paci, H. Santos and A. L. Maçanita, *Biophys. J.*, 2007, **92**, 4401–4414.

46 J. Santoro, C. Gonzales, M. Bruix, J. L. Neira, J. L. Nieto, J. Herranz and M. Rico, *J. Mol. Biol.*, 1993, 229, 722–734.

47 K. J. Willis and A. G. Szabo, *J. Phys. Chem.*, 1991, **95**, 1585–1589.

48 T. G. Flick, S. I. Merenbloom and E. R. Williams, *J. Am. Soc. Mass Spectrom.*, 2013, **24**, 1654–1662.

49 S. I. Merenbloom, T. G. Flick, M. P. Daly and E. R. Williams, *J. Am. Soc. Mass Spectrom.*, 2011, **22**, 1978–1990.

50 L. Han, S. J. Hyung, J. J. S. Mayers and B. T. Ruotolo, *J. Am. Chem. Soc.*, 2011, **133**, 11358–11367.

51 L. Han, S.-J. Hyung and B. T. Ruotolo, *Angew. Chemie Int. Ed.*, 2012, **51**, 5692–5695.

52 S. J. Allen, K. Giles, T. Gilbert and M. F. Bush, *Analyst*, 2016, **141**, 884–891.

53 D. Morsa, V. Gabelica and E. De Pauw, *J. Am. Soc. Mass Spectrom.*, 2014, **25**, 1384–1393.

54 R. L. Baldwin, C. Frieden and G. D. Rose, *Proteins Struct. Funct. Bioinforma.*, 2010, **78**, 2725–2737.

55 D. E. Clemmer, D. H. Russell and E. R. Williams, *Acc. Chem. Res.*, 2017, **50**, 556–560.

56 H. J. Sterling, A. F. Kintzer, G. K. Feld, C. A. Cassou, B. A. Krantz and E. R. Williams, *J. Am. Soc. Mass Spectrom.*, 2012, **23**, 191–200.

55 Native Mass Spectrometry of Membrane Proteins in Physiological Salts Preserve Binding of Endogenous Lipids, M. T. Agasid, I, Liko, J, Gault, C. V. Robinson, Citation # 293014, Jun 4th, *Proceedings of the 66th ASMS Conference on Mass Spectrometry and Allied Topic*, San Diego, CA,Jun 3rd to Jun 7th, 2018.

56 Is Native Mass Spectrometry Really Native? Comparisons of Protein Structures in Ammonium Acetate and in Common Biochemical Buffers, Z. Xia, J. B.

DeGrandchamp, E. R. Williams, Citation # 295392, Jun 4th, *Proceedings of the 66th ASMS Conference on Mass Spectrometry and Allied Topic*, San Diego, CA,Jun 3rd to Jun 7th, 2018.

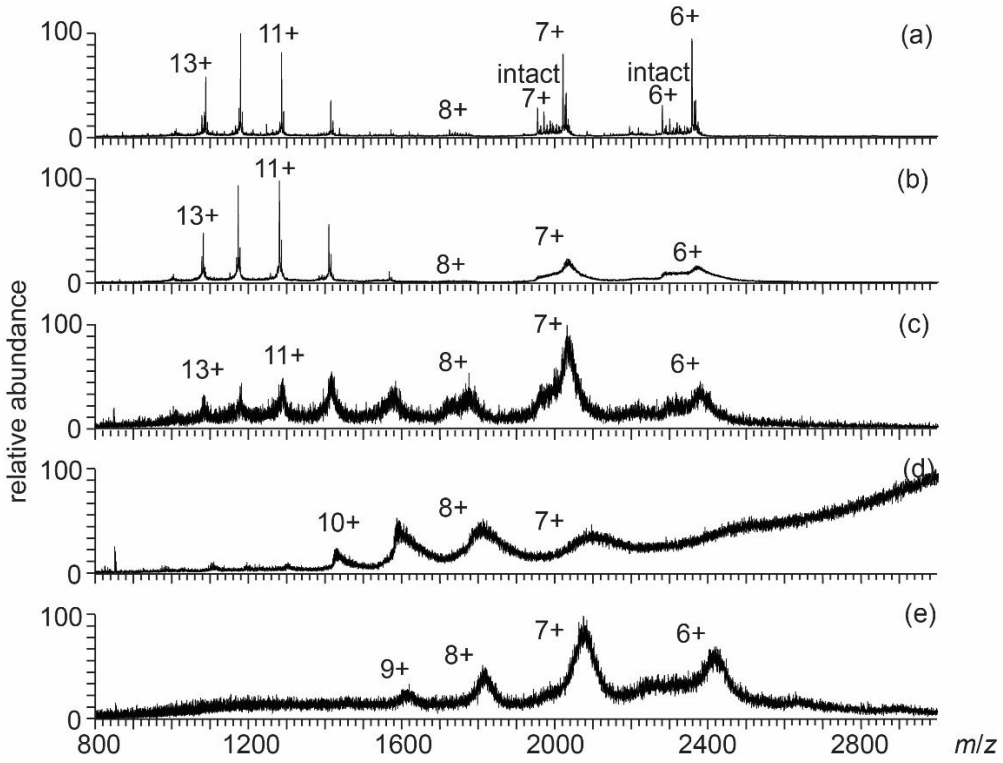

Figure 1. Electrospray ionization mass spectra of reduced RNase A in (a) 175 mM AA, (b) 165 mM AA and 10 mM NaCl, (c) 125 mM AA and 50 mM NaCl, (d) 25 mM AA and 150 mM NaCl, and (e) 25 mM Tris and 150 mM NaCl at pH 6.8. A small abundance of intact RNase A appears at lower charge state (6+ and 7+).

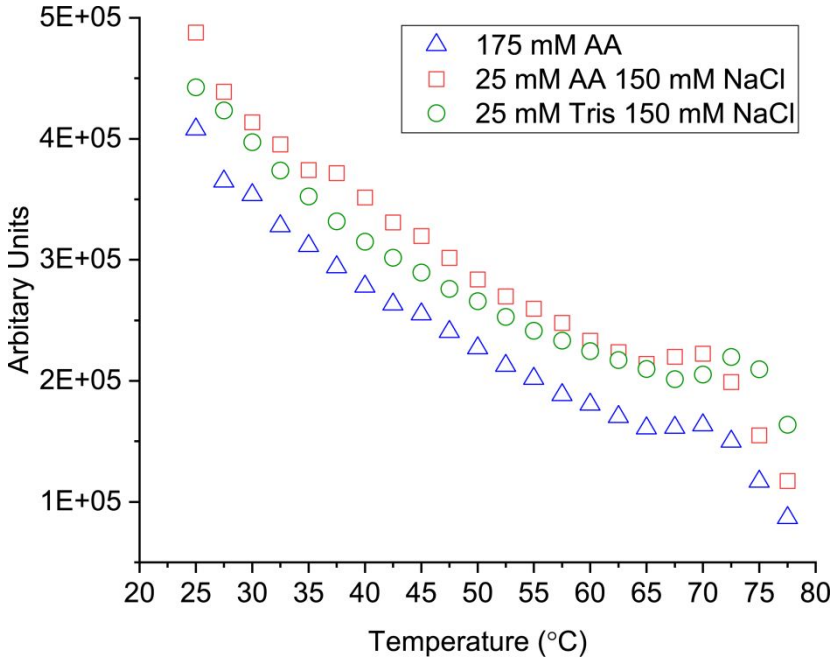

Figure 2. Tyrosine emission intensity at 302 nm as a function of temperature for RA-RNase A in 175 mM AA (black square), in 25 mM AA 150 mM NaCl (red circle), and in 25 mM Tris 150 mM NaCl (green triangle) solutions. The sample is excited at 280 nm.

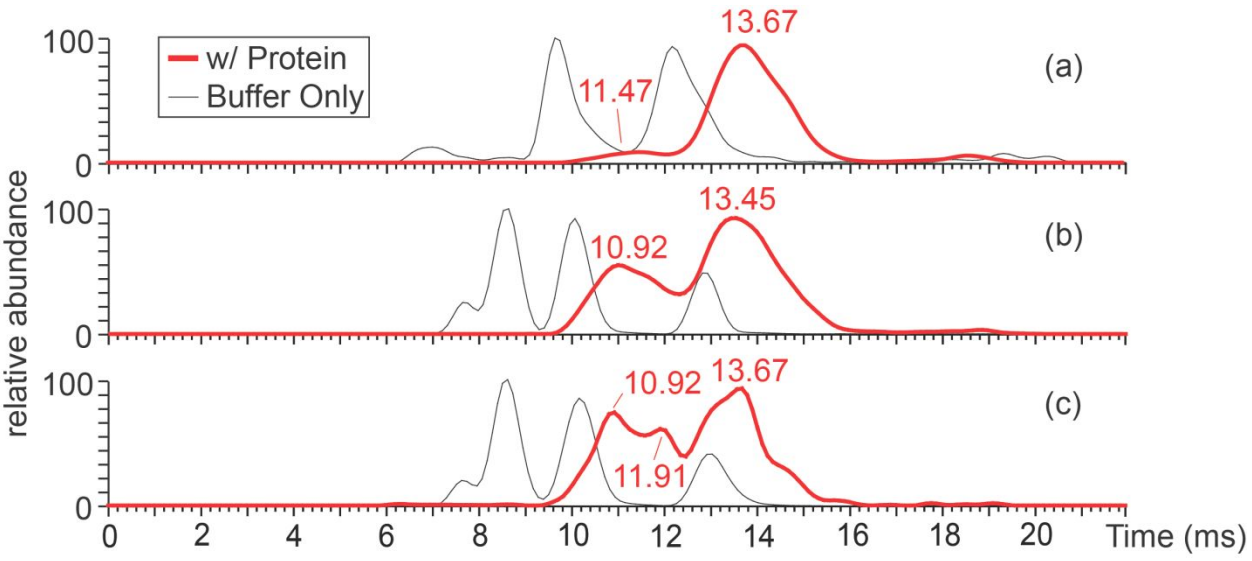

Figure 3. Ion mobility arrival time data for RA-RNase A 7+ (*m*/*z* 2020.5 – 2028.5) in (a) 175 mM AA, (b) in 165 mM AA 10 mM NaCl, and (c) in 125 mM Tris 50 mM NaCl solutions. Data for the 7+ ion of RA-RNase A (red) are overlaid with data from

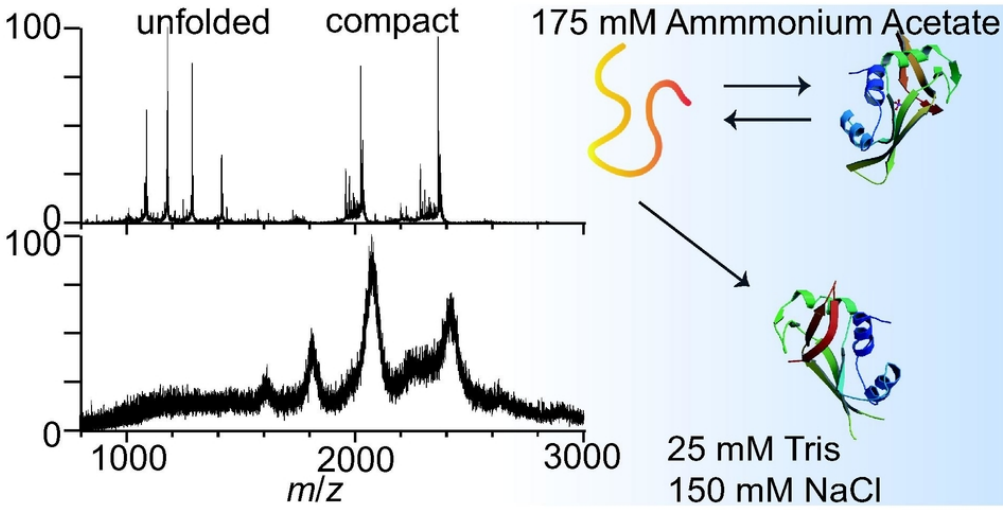

79x40mm (300 x 300 DPI)